Electronic Supplementary Information

Metal organic framework-derived CoPS/N-doped carbon for efficient electrocatalytic hydrogen evolution

Yuzhi Li,[a] Siqi Niu,[a] Dmitrii Rakov,[a] Ying Wang,[a] Miguel Cabán-Acevedo,[b] Shijian Zheng,[c] Bo Song*[d] and Ping Xu*[a]

[a.] MIIT Key Laboratory of Critical Materials Technology for New Energy Conversion and Storage, School of Chemistry and Chemical Engineering, Har-bin Institute of Technology, Harbin 150001, China. Email: pxu@hit.edu.cn

[b.] Department of Chemistry, University of Wisconsin–Madison, 1101 University Avenue, Madison, Wisconsin 53706, USA.

[c.] Shenyang National Laboratory for Materials Science, Institute of Metal Research, Chinese Academy of Sciences, Shenyang 110016, China.

[d.] Academy of Fundamental and Interdisciplinary Sciences, Department of Physics, Harbin Institute of Technology, Harbin 150001, China. Email: songbo@hit.edu.cn

Supplementary Figures and Tables

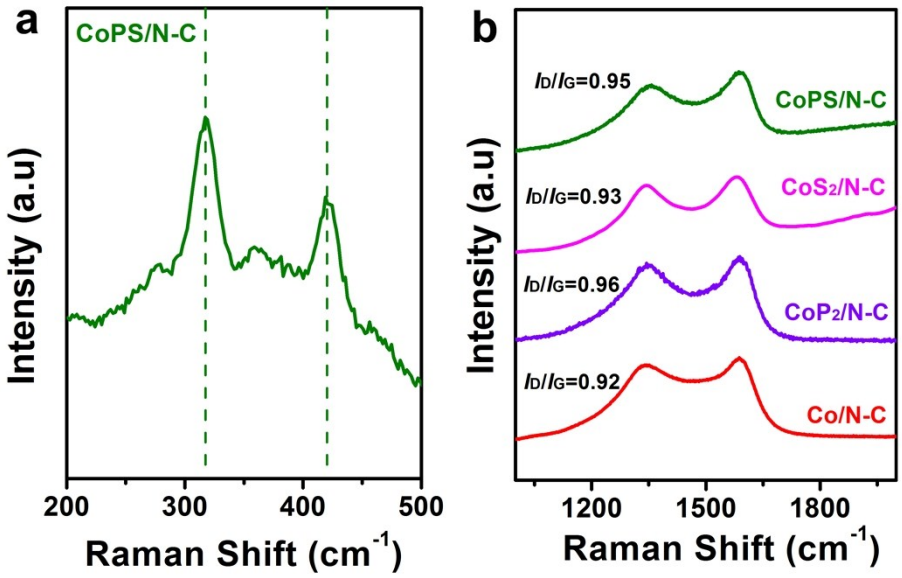

Fig. S1. Raman spectra of the Co/N-C, CoPS/N-C, CoP_2/N-C and CoS_2/N-C nanocomposites. (a) Raman feature of CoPS/N-C nanocomposites in the region of 200-500 cm^{-1}, where two typical peaks at ~322 and 427 cm^{-1} correspond to the characteristic active modes of vibration (E_g) and in-phase stretching (A_g) for the chalcogenide dumbbells in a pyrite crystal lattice. (b) Raman feature in the region showing the D band and G band of carbon materials. The intensity ratios of D band and G band (I_D/I_G) are almost identical, an indication that the graphitization degrees of the carbon materials in these nanocomposites are similar for the Co/N-C, CoPS/N-C, CoP_2/N-C and CoS_2/N-C nanocomposites.

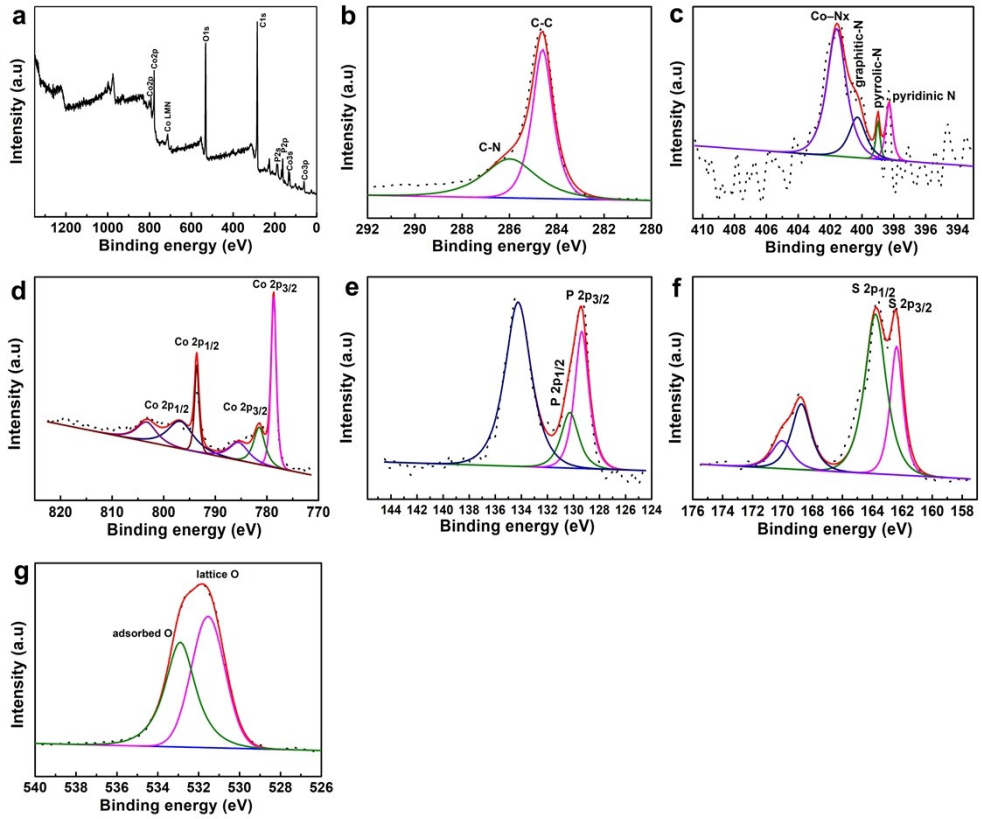

Fig. S2. Survey XPS spectrum (a), and high-resolution XPS spectra of (b) C 1s, (c) N 1s, (d) Co 2p, (e) P 2p, (f) S 2p and (g) O 1s levels of CoPS/N-C nanocomposites.

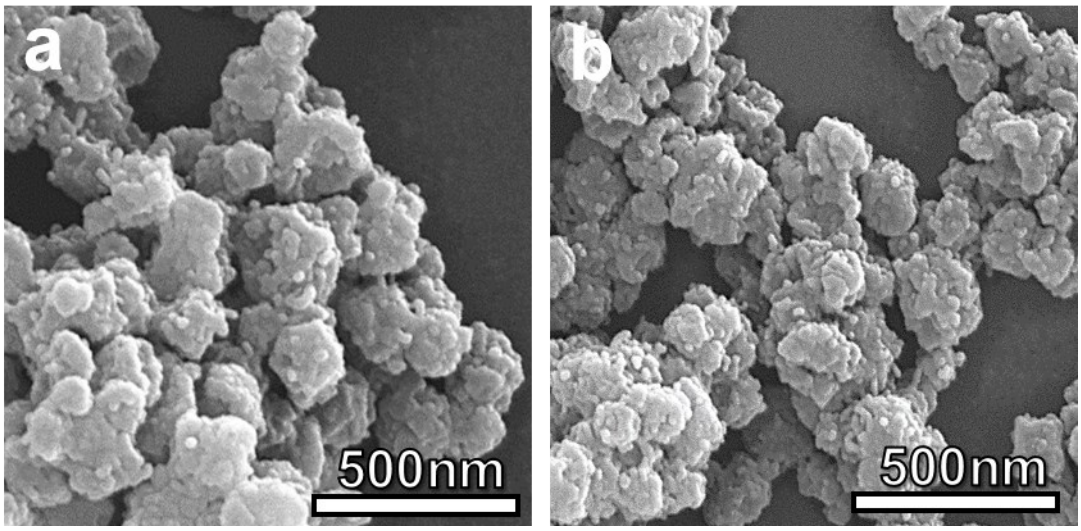

Fig. S3. SEM images of (a) CoP_2/N-C and (b) CoS_2/N-C nanocomposites. The nanocomposites inherited the overall polyhedron-like morphology of ZIF-67 and have nanoparticle formation at the surface of CoP_2/N-C and CoS_2/N-C nanocomposites.

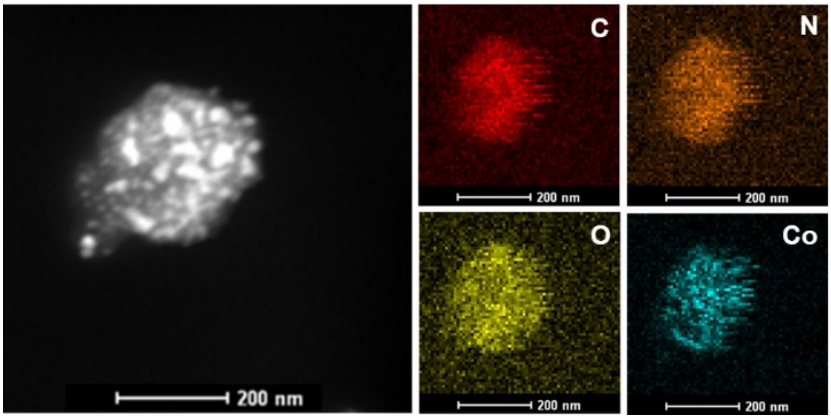

Fig. S4. STEM image of a single Co/N-C particle and the corresponding EDX elemental mapping of C, N, O and Co elements.

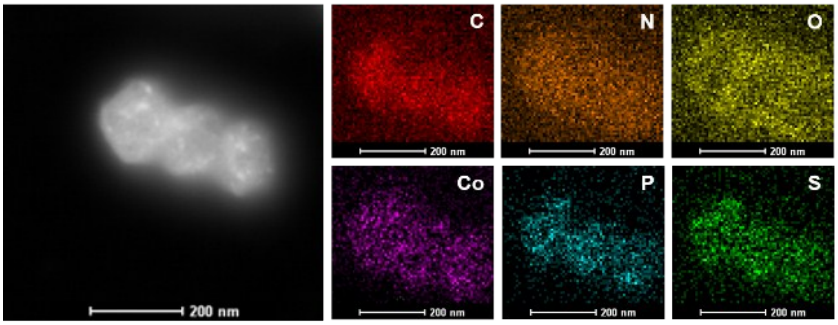

Fig. S5. STEM image of a single CoPS/N-C particle and the corresponding EDX elemental mapping of C, N, O, Co, P and S.

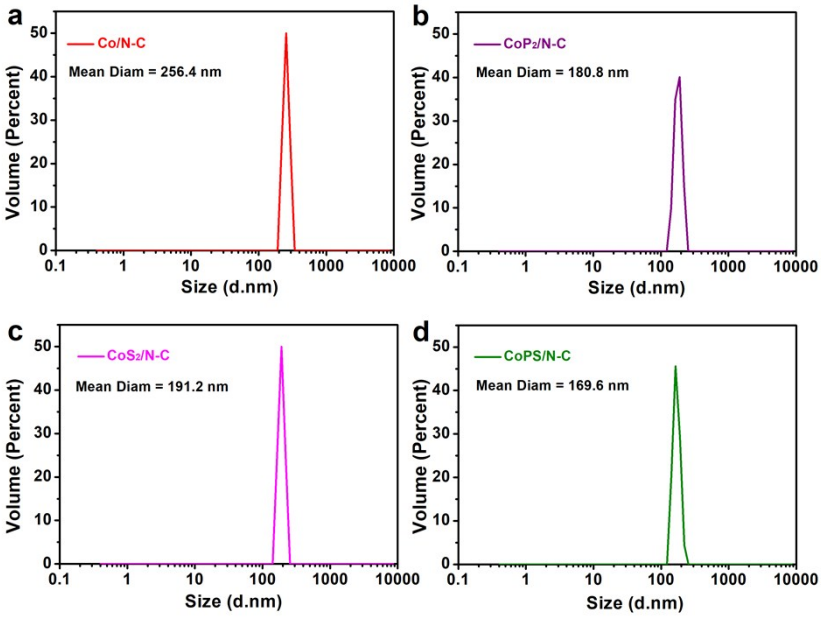

Fig. S6. Particle size distributions of the Co/N-C (a), CoP_2/N-C(b), CoS_2/N-C (c) and CoPS/N-C(d) suspended in water as determined by dynamic light scattering (DLS). Here, measured particle size distributions of Co/N-C, CoP_2/N-C, CoS_2/N-C and CoPS/N-C are 256.4 nm, 180 nm, 191.2 nm and 169.4 nm respectively.

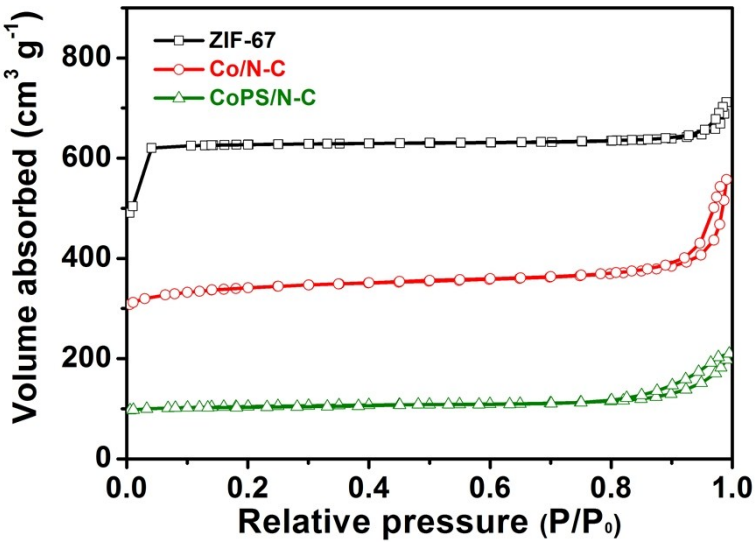

Fig. S7. N_2 adsorption-desorption isotherms of ZIF-67, Co/N-C and CoPS/N-C nanocomposites.

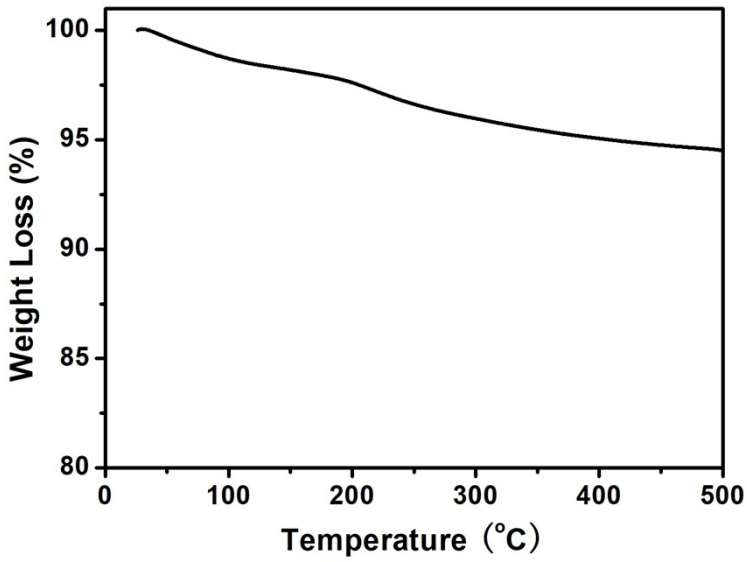

Fig. S8. Thermogravimetric curve of CoPS/N-C nanocomposites in N_2 atmosphere.

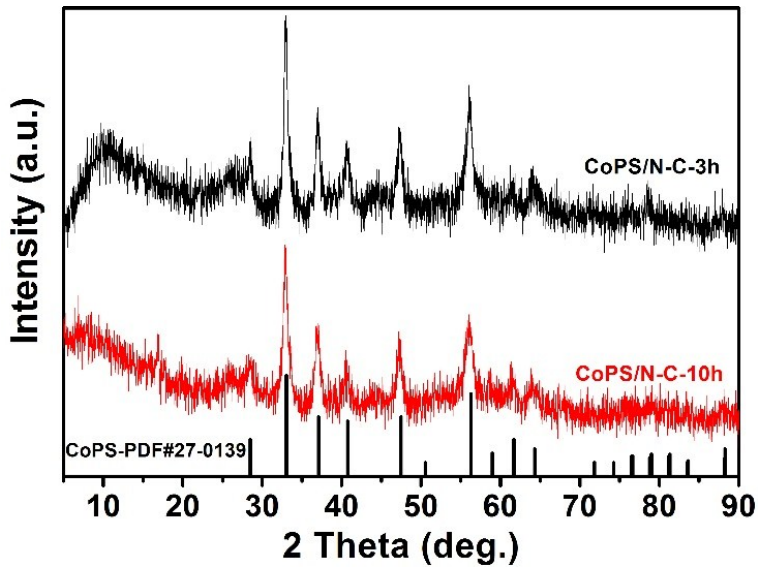

Fig. S9. XRD patterns of the CoPS/N-C nanocomposites prepared through a vacuum annealing process for 3 h and 10 h. CoPS phase can be formed in this shorter time annealing process, but the crystallinity is relatively low.

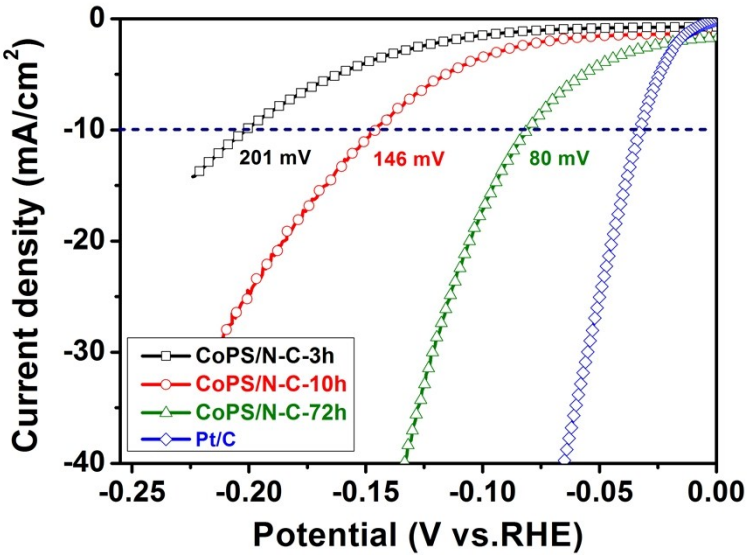

Fig. S10. Polarization curves after iR correction of CoPS/N-C nanocomposites prepared from different time periods (3 h, 10 h, and 72 h) for HER catalysis in 0.5 M H_2SO_4, in comparison to Pt/C.

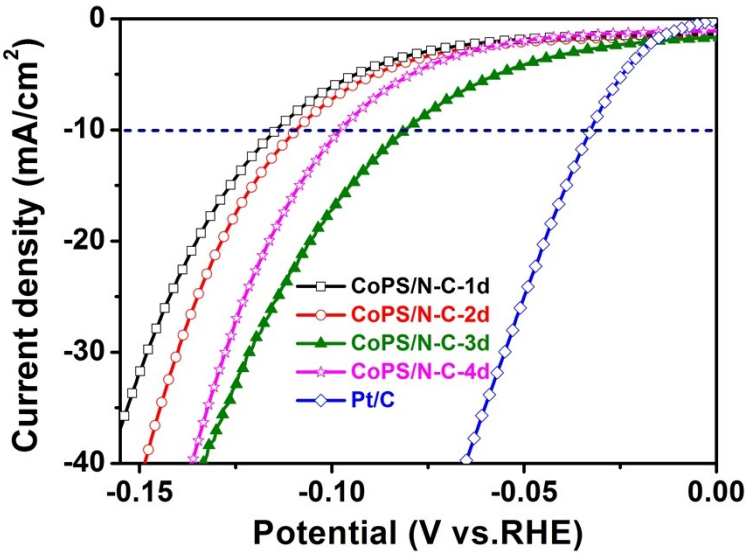

Fig. S11. Polarization curves after iR correction of CoPS/N-C nanocomposites prepared from different time periods (1 d, 2 d, 3 d, and 4 d) for HER catalysis in 0.5 M H_2SO_4, in comparison to Pt/C.

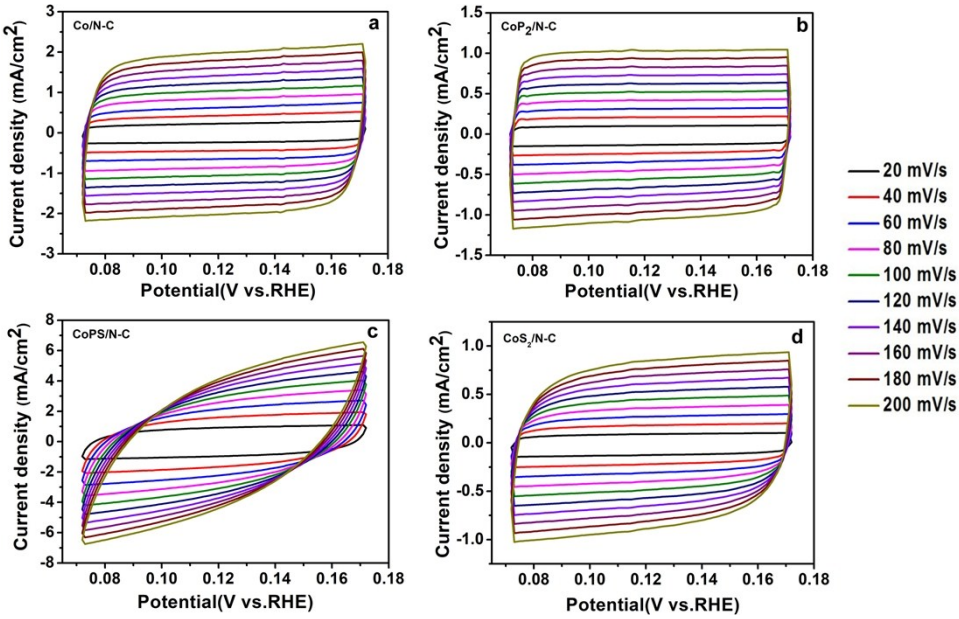

Fig. S12. Cyclic voltammetry curves of the Co/N-C, CoP_2/N-C, CoS_2/N-C and CoPS/N-C samples under different scan rates, in the region of 0.073-0.173V vs. RHE. These data were used to present the plots showing the extraction of the C_{dl} for different samples shown in Fig. 3c in the main text.

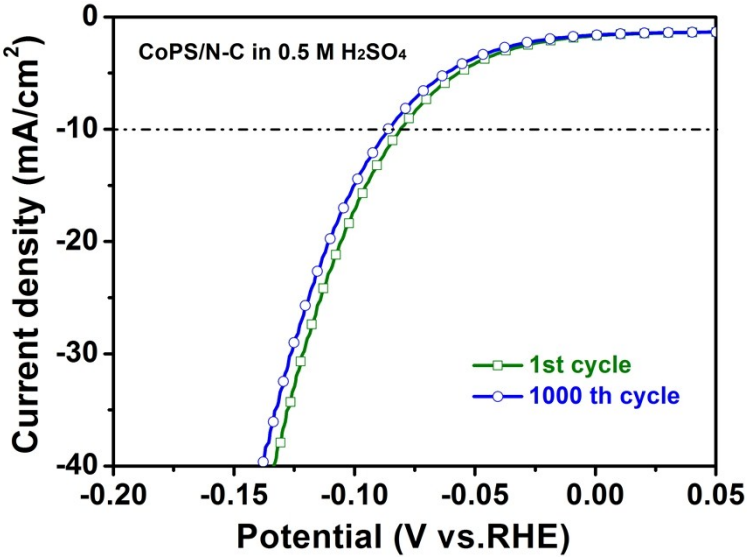

Fig. S13. Polarization curves of CoPS/C Nanocomposites as an HER catalyst in 0.5 M H_2SO_4 at the 1st cycle and 1000th cycle. After continuous cyclic voltammetry (CV) for 1000 cycles at a scan rate of 50 mV s^{-1}, the polarization curve for the CoPS/N-C shows a very slight change, where η_{10} can still be maintained at -85 mV vs RHE.

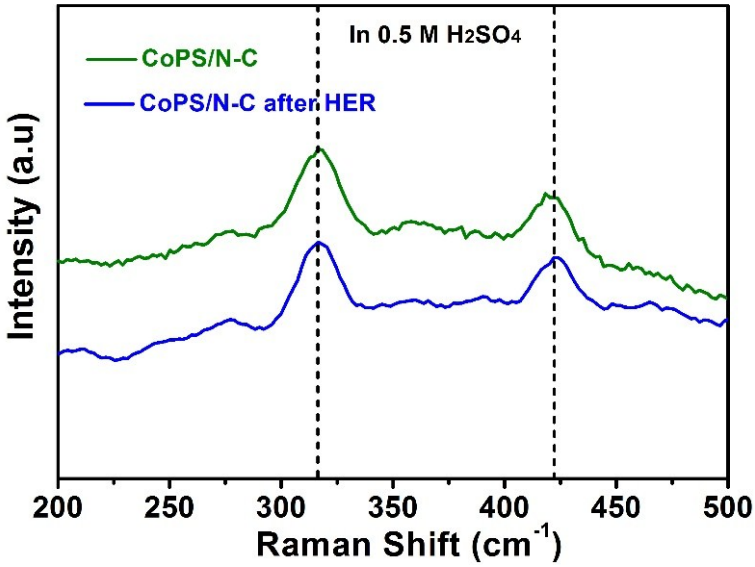

Fig. S14. Raman spectra of CoPS/N-C nanocomposites before and after 1,000 cycles of HER in 0.5 M H_2SO_4 solution. No obvious structural or compositional change during the course of HER in acidic medium, which confirms the high stability of CoPS/N-C nanocomposites for HER catalysis.

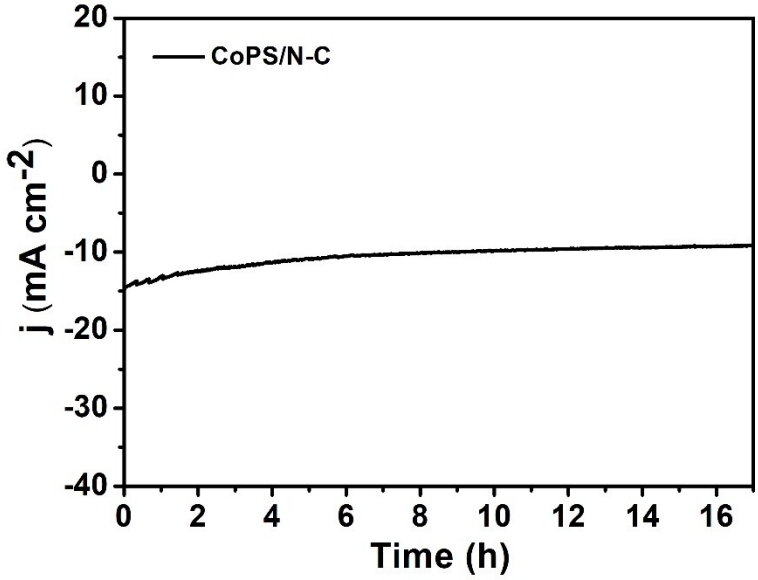

Fig. S15. Stability of CoPS/N-C nanocomposites as an HER catalyst in acidic media. Time-dependent current density under a constant overpotential of 80 mV vs RHE. The current density exhibits negligible degradation even after a long period of 16 h.

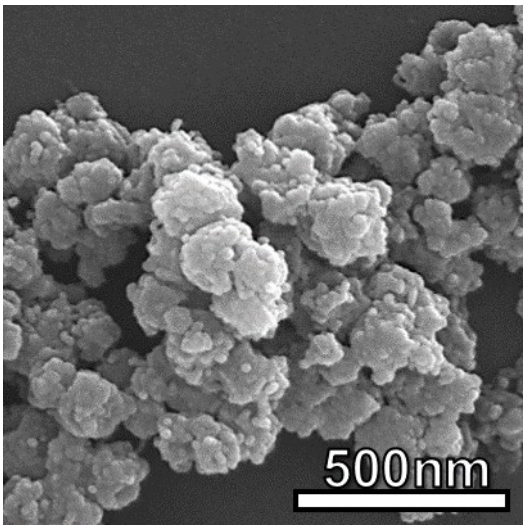

Fig. S16. SEM images of CoPS/N-C nanocomposites after it test. No obvious change in the size and morphology of the CoPS/N-C after the *i-t* test could be seen, confirming the robustness as a highly active HER electrocatalyst.

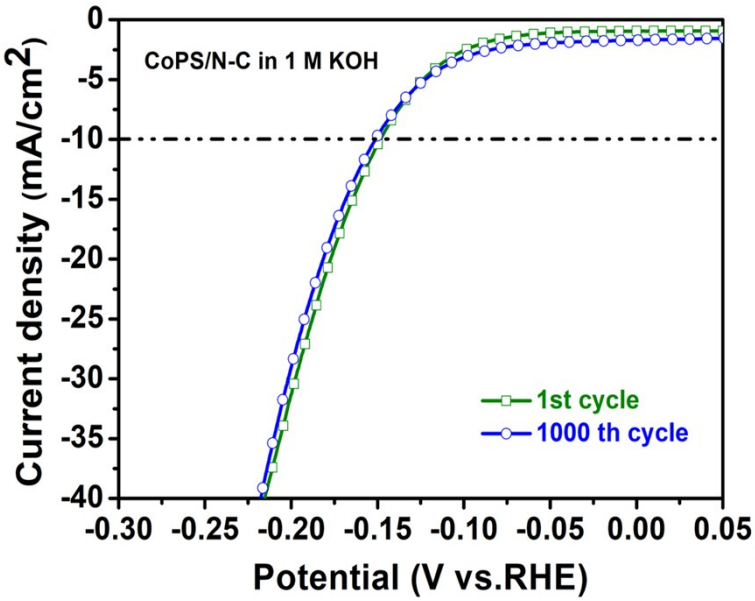

Fig. S17. Polarization curves of CoPS/C Nanocomposites as an HER catalyst in 1 M KOH at the 1st cycle and 1000th cycle. After continuous cyclic voltammetry (CV) for 1000 cycles at a scan rate of 50 mV s^{-1}, the polarization curve for the CoPS/N-C shows a very slight change, where η_{10} can still be maintained at -150 mV vs RHE.

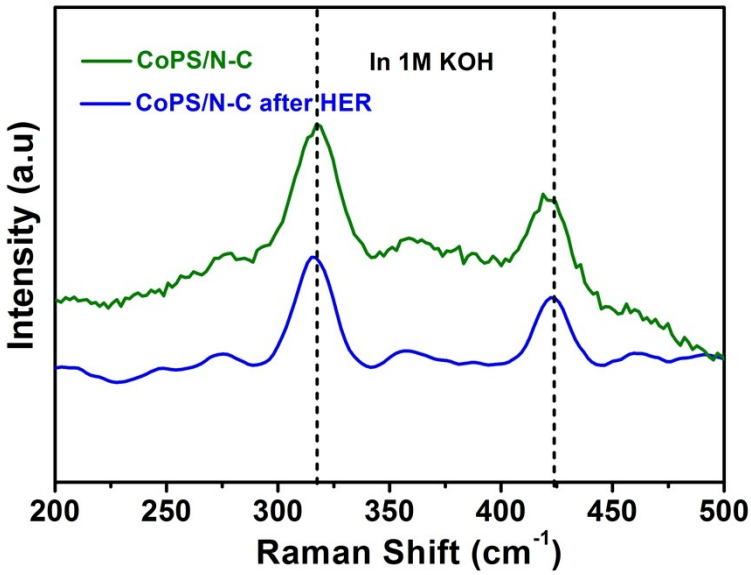

Fig. S18. Raman spectra of CoPS/N-C nanocomposites before and after 1,000 cycles of HER in 1 M KOH solution.

Table S1 Summary of the elemental contents of CoPS/N-C nanocomposites.

Sample	element contents / (at%)					
	C	N	O	Co	P	S
CoPS/N-C	56.71	4.91	7.02	10.9	10.18	10.28

Table S2 BET surface areas and adsorption total pore volumes of ZIF-67, Co/N-C and CoPS/N-C nanocomposites.

Sample	BET surface area (m^2 g^{-1})	Pore volume (cm^3 g^{-1})
ZIF-67	1493.08	0.77
Co/N-C	317.21	0.28
CoPS/N-C	69.02	0.13

Table S3 Comparative characteristics of HER activity on different transition metal-based catalysts in acidic and alkaline media.

	0.5 M H_2SO_4		1 M KOH		
Catalyst	**η_{10} (mV *vs* RHE)**	**Tafel slope (mV dec^{-1})**	**η_{10} (mV *vs* RHE)**	**Tafel slope (mV dec^{-1})**	**ref.**
CoPS/N-C	80	68	148	78	This work
Co-P/NC			191	51	[1]
CoP hollow polyhedron	159	59			[2]
CoP particles	355	77			[2]
CoP NRAs	181	69			[3]
CoP/rGO-400	105	50	150	38	[4]
CoP@BCN	87	46	215	25	[5]
CoP-CNTs	139	52			[6]
CoP CPHs	133	51			[7]
CoP-N-C-400	91	42			[8]
CoP_3 CPs	78	53	124	88	[8]
Ni-P	110	73			[9]
Ni_2P	172	62			[10]
Fe_xP@NPC	227	81			[11]
FeP@PC	52	49			[12]
MoP@PC	47	45			[12]
MoP/SN-650	104	45			[13]
MoP@PC	153	66			[14]
MoS_2@TiO_2	340	81			[15]
NiS-100 nm			94	139	[16]
NiS-300 nm			115	131	
NiS-600 nm			148	141	
$CoSe_2$@DC	132	82			[17]
MoC_x	142	53	151	59	[18]
Ni-Co-P			150	60.1	[19]
NiCoP			133	68.6	[20]
$Co_{0.38}Fe_{0.62}P$	107	60	124	78	[21]
$Co_{0.59}Fe_{0.41}P$	72	52	92	72	[21]
$Co_{0.71}Fe_{0.29}P$	98	53	111	77	[21]
$Zn_{0.30}Co_{2.70}S_4$	80	47.5	85	60	[22]
NiPS3	530	56			[23]
CoPS3	580	84			[23]
FePS3	860	200			[23]

References

1. B. You, N. Jiang, M. Sheng, S. Gul, J. Yano and Y. Sun, *Chemistry of Materials*, 2015, **27**, 7636-7642.
2. M. Liu and J. Li, *ACS Appl Mater Interfaces*, 2016, **8**, 2158-2165.
3. L. Li, X. Li, L. Ai and J. Jiang, *RSC Adv.*, 2015, **5**, 90265-90271.
4. L. Jiao, Y.-X. Zhou and H.-L. Jiang, *Chem. Sci.*, 2016, **7**, 1690-1695.
5. H. Tabassum, W. Guo, W. Meng, A. Mahmood, R. Zhao, Q. Wang and R. Zou, *Advanced Energy Materials*, 2017, **7**, 1601671.
6. C. Wu, Y. Yang, D. Dong, Y. Zhang and J. Li, *Small*, 2017, **13**.
7. M. Xu, L. Han, Y. Han, Y. Yu, J. Zhai and S. Dong, *J. Mater. Chem. A*, 2015, **3**, 21471-21477.
8. T. Wu, M. Pi, X. Wang, D. Zhang and S. Chen, *Phys. Chem. Chem. Phys.*, 2017, **19**, 2104-2110.
9. X.-Y. Yu, Y. Feng, B. Guan, X. W. Lou and U. Paik, *Energy Environ. Sci.*, 2016, **9**, 1246-1250.
10. M. Ledendecker, S. Krick Calderon, C. Papp, H. P. Steinruck, M. Antonietti and M. Shalom, *Angew Chem Int Ed Engl*, 2015, **54**, 12361-12365.
11. Y. Cheng, J. Guo, Y. Huang, Z. Liao and Z. Xiang, *Nano Energy*, 2017, **35**, 115-120.
12. S. Han, Y. Feng, F. Zhang, C. Yang, Z. Yao, W. Zhao, F. Qiu, L. Yang, Y. Yao, X. Zhuang and X. Feng, *Advanced Functional Materials*, 2015, **25**, 3899-3906.
13. M. A. R. Anjum and J. S. Lee, *ACS Catalysis*, 2017, **7**, 3030-3038.
14. J. Yang, F. Zhang, X. Wang, D. He, G. Wu, Q. Yang, X. Hong, Y. Wu and Y. Li, *Angew Chem Int Ed Engl*, 2016, **55**, 12854-12858.
15. B. Ma, P. Y. Guan, Q. Y. Li, M. Zhang and S. Q. Zang, *ACS Appl Mater Interfaces*, 2016, **8**, 26794-26800.
16. X. Y. Yu, L. Yu, H. B. Wu and X. W. Lou, *Angew Chem Int Ed Engl*, 2015, **54**, 5331-5335.
17. M. Jiang, Y. J. Li, Z. Y. Lu, X. M. Sun and X. Duan, *Inorg. Chem. Front.*, 2016, **3**, 630-634.
18. H. B. Wu, B. Y. Xia, L. Yu, X. Y. Yu and X. W. Lou, *Nat Commun*, 2015, **6**, 6512.
19. Y. Feng, X. Y. Yu and U. Paik, *Chem Commun (Camb)*, 2016, **52**, 1633-1636.
20. Y. Li, H. Zhang, M. Jiang, Y. Kuang, X. Sun and X. Duan, *Nano Research*, 2016, **9**, 2251-2259.
21. J. Hao, W. Yang, Z. Zhang and J. Tang, *Nanoscale*, 2015, **7**, 11055-11062.
22. Z. F. Huang, J. Song, K. Li, M. Tahir, Y. T. Wang, L. Pan, L. Wang, X. Zhang and J. J. Zou, *J Am Chem Soc*, 2016, **138**, 1359-1365.
23. C. C. Mayorga-Martinez, Z. Sofer, D. Sedmidubsky, S. Huber, A. Y. Eng and M. Pumera, *ACS Appl Mater Interfaces*, 2017, **9**, 12563-12573.